

# We are IntechOpen, the world's leading publisher of Open Access books Built by scientists, for scientists

6,900

Open access books available

186,000

International authors and editors

200M

Downloads

Our authors are among the

154

Countries delivered to

TOP 1%

most cited scientists

12.2%

Contributors from top 500 universities



WEB OF SCIENCE™

Selection of our books indexed in the Book Citation Index  
in Web of Science™ Core Collection (BKCI)

Interested in publishing with us?  
Contact [book.department@intechopen.com](mailto:book.department@intechopen.com)

Numbers displayed above are based on latest data collected.  
For more information visit [www.intechopen.com](http://www.intechopen.com)



# The Detection Data of Mammary Carcinoma Processing Method Based on the Wavelet Transformation

Meng Yao,  
Zhifu Tao and Zhongling Han  
*East China Normal University  
P. R. China*

## 1. Introduction

At present, breast cancer is one of the major threaten diseases for female(Xu & Tang, 1996). Microwave breast tumor detection will be the future development direction of clinical diagnostic, as a safe, mobile and cost-effective method, and the hotspot of breast cancer non-invasive diagnosis for decades. Unlike traditional diagnostic method of soft X-ray mammography imaging, microwave near-field tomography is a safe method of imaging diagnosis of breast tumor which is very low damage when detect on the human body. From the perspective of breast tumors medical imaging diagnosis, it is required for the target location on the contour (line) information or hierarchical information. The imaging information of medical diagnosis of mammary tumor in early stage bases on the great different between the dielectric properties of the normal breast tissues and the malignant ones. Therefore, when the electromagnetic wave enters the malignant tumor tissues from the normal mammary tissues, it will interact with the media (for example, absorption, dispersion, emission, etc.), and then the electromagnetic wave transmission path is changed. The electric-field intensity and the magnetic field strength is enhanced in certain regions, while is weakened in other regions. Based on this characteristic, mammary gland tumors can be detected by surveying the electrical field which is produced by the reflection and the scattering generated by near-field microwave. This method can facilitate the early discovery of cancer, early identification of treatment programs and achieve early medical imaging diagnosis of breast cancer. The signals obtained by Breast Tumor Microwave Sensor System (BRATUMASS) are non-linear and non-steady. So the analysis of the detected signals is significantly important for detecting and diagnosing of the early-stage breast tumor. Delays of backscattering in cancerous tissue surfaces are different, for the dissimilar possible location of the cancerous tissue and the different distance from detecting point to cancerous tissue. The different delays can make the equivalent frequency emerge in anywhere of the effective frequency range of system. Moreover, backscattering occurs in other tissues surface. These aspects increase the frequency component and the difficulties of analysis. Fig. 1 shows the typical signal obtained from one detecting point.

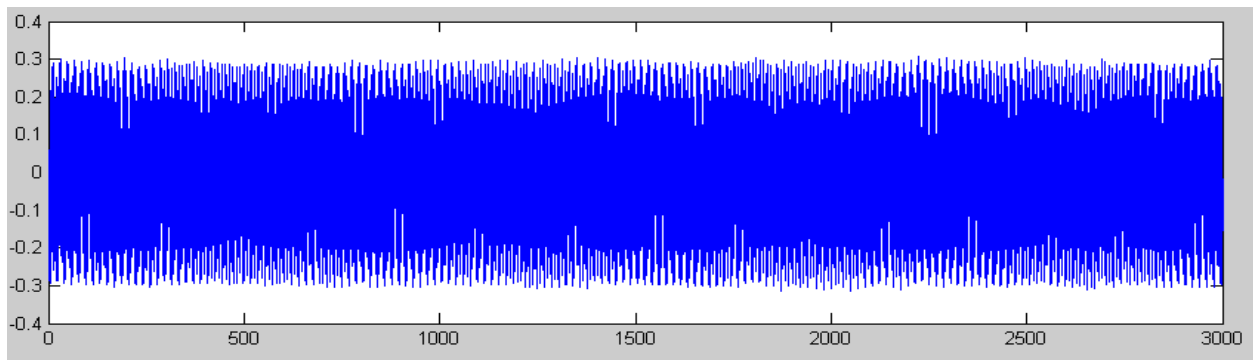


Fig. 1. Typical signal obtained from one detecting point. X-coordinate is the number of data, Y-coordinate is voltage, unit V. sampling interval is 0.002 s and sampling depth is 3000

## 2. The principle of detection system

Breast tumor microwave sensor system (BRATUMASS) consists of RF transceiver module, zero intermediate frequency (zero-IF) mixer. In the transmission, we use slot step frequency modulation method. In the receiver, we sample from zero IF output. In detection process, we arrayed the transceiver (R/T) antenna testing points around the test region and each sounding point of surface-wave (sagittal). There are 12 or 16 detection points of antenna devices, during the real detection process. The area enclosed by circular dashed line is the detected region. Figure 2 shows the block diagram of BRATUMASS.

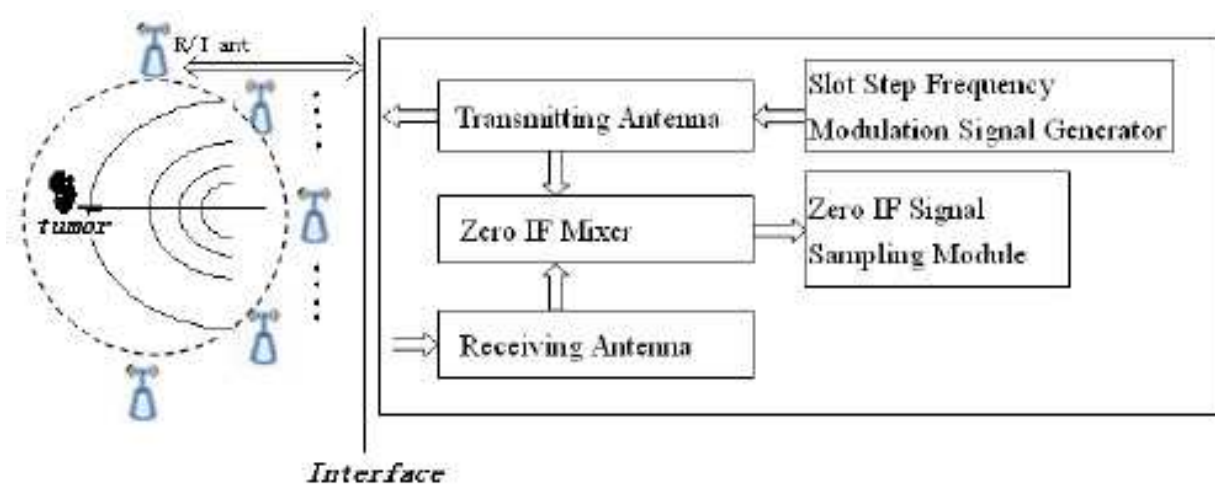


Fig. 2. Block diagram of BRATUMASS

For the large difference of dielectric properties between breast tissue and malignant tumor tissue, scattering will be happened in the interface of breast tissue and malignant tumor tissue. Figure 3 shows the relationship of reflection and transmission at the two different mediums interface. Where  $P_i$  is incident power,  $P_r$  is reflected power,  $P_t$  is transmitted power.

In two non-magnetic medium interface, the relationship between reflection coefficient  $\Gamma_{i,j}$  and dielectric properties  $\epsilon_1, \epsilon_2$  is:

$$\Gamma_{i,j} = \frac{\sqrt{\epsilon_2} - \sqrt{\epsilon_1}}{\sqrt{\epsilon_2} + \sqrt{\epsilon_1}} \quad (1)$$

The ratio of incident power to reflected power is:

$$\frac{P_r}{P_i} = |\Gamma_{i,j}|^2 \quad (2)$$

In each detecting, the location of the target and the transceiver are relatively fixed, so the frequency components of low-frequency signal output by zero-IF mixer are relatively fixed too. Extracted the power spectrum of zero-IF output low-frequency signal to decide the target corresponding reflection coefficient.(Fourier diffraction relationship)

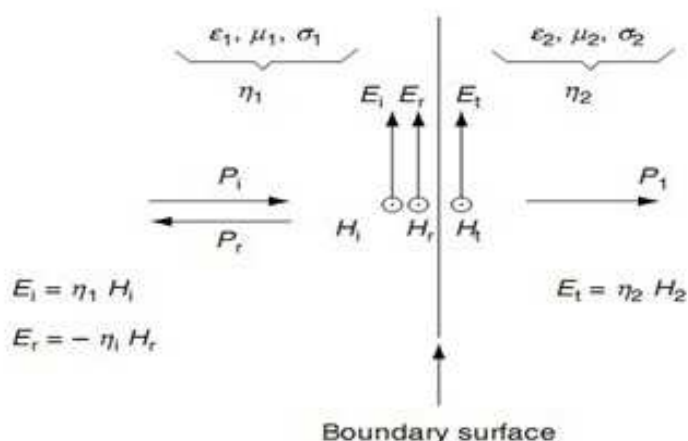


Fig. 3. Reflection and transmission of an microwave wave at the two different mediums interface. Pi = incident power, Pr = reflected power, Pt = transmitted power.

The collection reflection coefficient  $\tilde{\Gamma}_{i,j}$  for the N layer media is:

$$\tilde{\Gamma}_{i,i+1} = R_{i,i+1} + \frac{T_{i,i+1} \tilde{\Gamma}_{i+1,i+2} T_{i+1,i} e^{2ik_{i+1,z}(d_{i+1}-d_i)}}{1 - R_{i+1,i} \tilde{\Gamma}_{i+1,i+2} e^{2ik_{i+1,z}(d_{i+1}-d_i)}} \quad (3)$$

Using our device parameters (transmitting frequency is 1.575 GHz and bandwidth is 200 MHz ) to compute the parameter, we obtain dielectric properties , reflection coefficient and conductivity of the breast tissue as shown in table 1.

	Dielectric properties $\epsilon_r$	Reflection coefficient $\Gamma$	Conductivity $\sigma$ (S/m)
skin	36		2.64
normal breast tissue	10		0.24
malignant tumor tissue	50	0.49	2.8
mammary duct	11~14	0.2018~0.49	0.45
vascular		0.15~0.2018	

Table 1. Dielectric properties of typical breast tissues in 1.575GHz

The bandwidth of slot step frequency modulation emission signal is 200MHz, transmitting frequency 1.575GHz, scanning period 1ms. As shown in Figure 4(a), the real line stands for the transmitting signal and the dashed line for the theoretical receiving signal. The frequency of the scanning signal rises step by step. Figure 4(b) shows the zero-IF signal output from the mixer. IF contains the information for breast tumor location. The transmitting signal reaches the receiving antenna and mixer after being reflected by breast tumor, while the other part directly gets to the mixer through transmitting antenna coupling networks. The course difference of two parts, which can be deduced from zero-IF, the output of the mixer, is used to determine the distance between the antenna and the tumor.

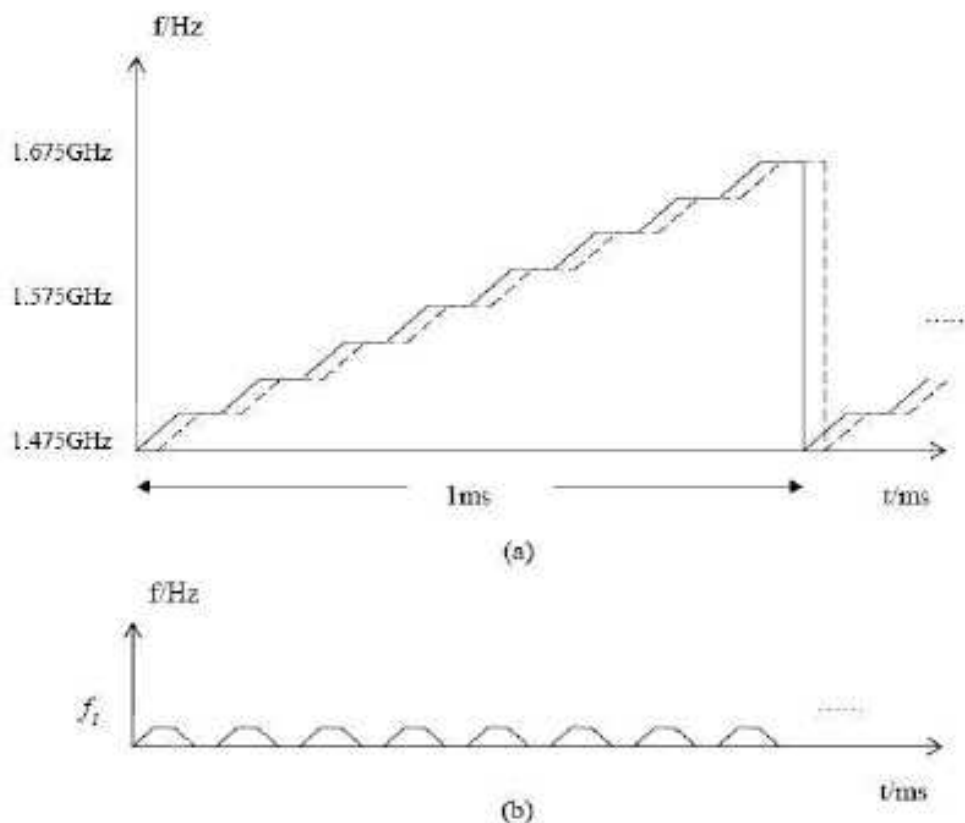


Fig. 4. Slot step frequency modulation signal.

(a) Real line stands for the transmitting signal, dashed line for the theoretical receiving signal (frequency --time)

(b) Zero-IF signal output (frequency --time)

Consider wave equation of the scattering field  $u_s(r)$ :

$$(\nabla^2 + k^2)u_s(r) = -k^2 f(r)u(r) \quad (4)$$

Where,  $u(r)$  is the wave function of incident wave,  $k$  is the wave number, and  $f(r)$  is the characteristic function of space scattering. The right of the equation is the source function of homogeneous medium in the spread of the scattering field  $u_s(r)$  with wave number  $k$ . this type equation solving can use Green's function. Considering the two-dimensional situation, the source of the radiation field of free space is located in the  $r_0 = (x_0, y_0)$ , Green's function is given by:

$$g(r_1 | r_0) = \frac{1}{4} H_0(k|r_1 - r_0|) \quad (5)$$

Where,  $H_0$  is the first zero-order Hankel function (that is the third type of Bessel function). By the principle of superposition, we can obtain the scattered field:

$$u_s(r) = \frac{ik^2}{4} \iint_S f(r_0)u(r_0)H_0(k|r - r_0|)dr_0 \quad (6)$$

Where S is the arbitrary area of surrounded objects cross-section in (x,y) plane. Also has:

$$H_0(k|r - r_0|) = \frac{1}{\pi} \int_{-\infty}^{\infty} \frac{1}{\beta} \exp\{i[\alpha(x - x_0) + \beta(y - y_0)]\} \quad (7)$$

In this equation,  $u(r)$  includes  $u_s(r)$ , so we can only obtain approximate solution. In the first-order Born approximation, scattering is weak, and we can use the incident field to instead of the total field. Then we can get:

$$u_s(r) = \frac{ik^2 u_0}{4\pi} \iint_S f(r_0) \exp(iks_0 \bullet r_0) \int_{-k}^k \frac{1}{\beta} \exp\{i[\alpha(x - x_0) + \beta(y - y_0)]\} d\alpha dr_0 \quad (8)$$

When the detector is located in  $y = l$ , the detector receiving scattering field is:

$$u_s(x, l) = \frac{ik^2 u_0}{4\pi} \int_{-k}^k d\alpha \frac{1}{\beta} \exp(i(\alpha x + \beta l)) \iint_S f(x_0, y_0) \exp\{-i[\alpha(x_0) + (\beta - k)y_0]\} dx_0 dy_0 \quad (9)$$

And

$$F(\omega_1, \omega_2) \Big|_{\substack{\omega_1 = \alpha \\ \omega_2 = \beta - k}} = F(\alpha, \beta - k) \quad (10)$$

Its also can be written as follows:

$$u_s(x, l) = \frac{ik^2 u_0}{4\pi} \int_{-k}^k \frac{1}{\beta} \exp(i(\alpha x + \beta l)) F(\alpha, \beta - k) d\alpha \quad (11)$$

$U_s(\omega)$  is the Fourier transform of one-dimensional function  $u_s(x, l)$  for the variable x, then:

$$U_s(\omega, l) = \frac{ik^2 u_0}{2} \frac{1}{\sqrt{k^2 - \omega^2}} \exp\left(i\sqrt{k^2 - \omega^2}l\right) F(\omega_1, \omega_2) \Big|_{\substack{\omega_1 = \omega \\ \omega_2 = \sqrt{k^2 - \omega^2} - k}}, \quad |\omega| < k \quad (12)$$

$F(\omega_1, \omega_2)$  is the Fourier transform of the space characteristics function  $f(x, y)$ . When  $\omega_1$  and  $\omega_2$  satisfied the relationship:

$$\omega_2 = \sqrt{k^2 - \omega_1^2} - k, \quad (13)$$

we can obtain the one-dimensional Fourier transform  $U_s(\omega, \cdot)$  of scattering measured data after properly weighted.

### 3. Description and mathematical model

We can obtain the sagittal distribution of the breast tissues dielectric properties from receiving signal. The sagittal distribution of the dielectric properties refers to the accumulated value of the dielectric properties along the arc circle whose center is the antenna. The sagittal of the arc circle varies from 0 to  $D$ , where  $D$  is the diameter of the target region. We have known the values of the dielectric properties along each arc circle. In the detection model, there are totally 12 or 16 antennas. For each antenna, the value of the dielectric properties along the arc circle can be calculated by the signal received from detection system. Now the problem is how to deduce the dielectric properties value of each point by the sagittal distribution.

As shown in Figure 5, dash-dotted frame is target region. We assume that the microwave reflection function in target region is  $\Gamma(x, y)$  which is bounded. We assume that there are  $N$  targets, recorded as  $M_i$  ( $i = 1, 2, \dots, n$ ) and  $P_j$  is the  $j$ th microwave detecting point. Where  $O$  is the coordinate center;  $L_i$  is the arc with center  $P_j$ , and radius  $r_i = P_j M_i$ .  $S_i$  is proportional to the integral of  $\Gamma(x, y)$  along the curve  $L_i$ , that is:

$$S_i(r_i) = \int_{L_i} \Gamma(x, y) dl . \quad (14)$$

Receiving signal is the sequence of  $S_1, S_2, \dots, S_n$ . BRATUMASS use the polar coordinate with  $P_j$  as the pole,  $P_j O$  as the polar. The target region used the Cartesian coordinate system. In practical calculation process, we need coordinate transformation.

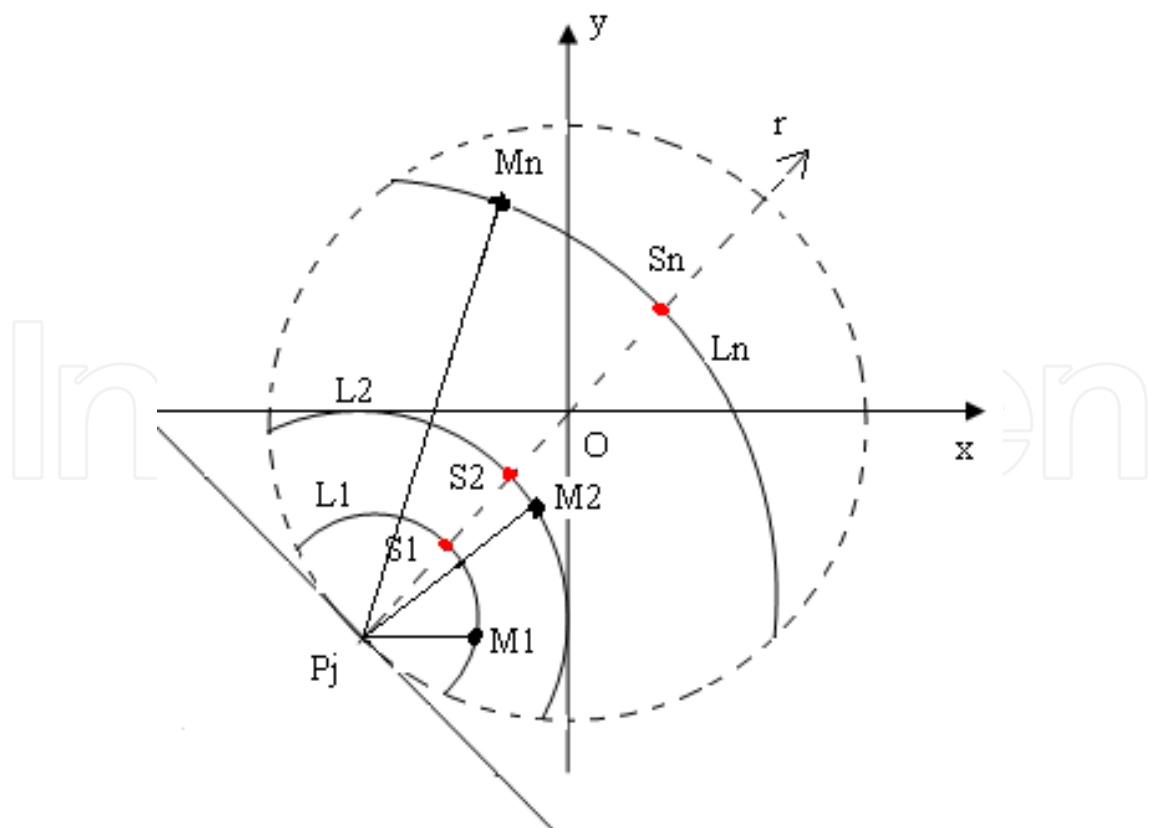


Fig. 5. Detection points and reflection interfaces

By Fourier diffraction theorem in microwave near field conditions, wave front projection is the system Fourier transforms. So back signal analysis is transformed the separation of projection data on different detecting arc. The detected target is manifested in the different duration of microwave transmission. In BRATUMASS, different time difference registers as the different frequencies outputting zero-IF signal. Sampling signal blend the reflections of all organization interfaces. Namely, the frequency components of sampling signal represent projection of all different detection arcs, and the back-wave's energy distribution relate to each reflection coefficient of detection arc.

All frequency components of back wave are decomposed by using Hilbert-Huang transform (HHT). This method based on empirical mode decomposition (EMD) and Hilbert transform (HT) is more suitable for analyzing nonlinear and non-stationary data than Fourier and wavelet method which depend on the priori function (Huang, N. E., etc.1998).

The high and low frequency components of zero-IF signal are output by HHT decomposition. Figure 6 is the EMD of each frequency component of one detection point outputted by zero-IF, Figure 7 is the corresponding FFT transformation.

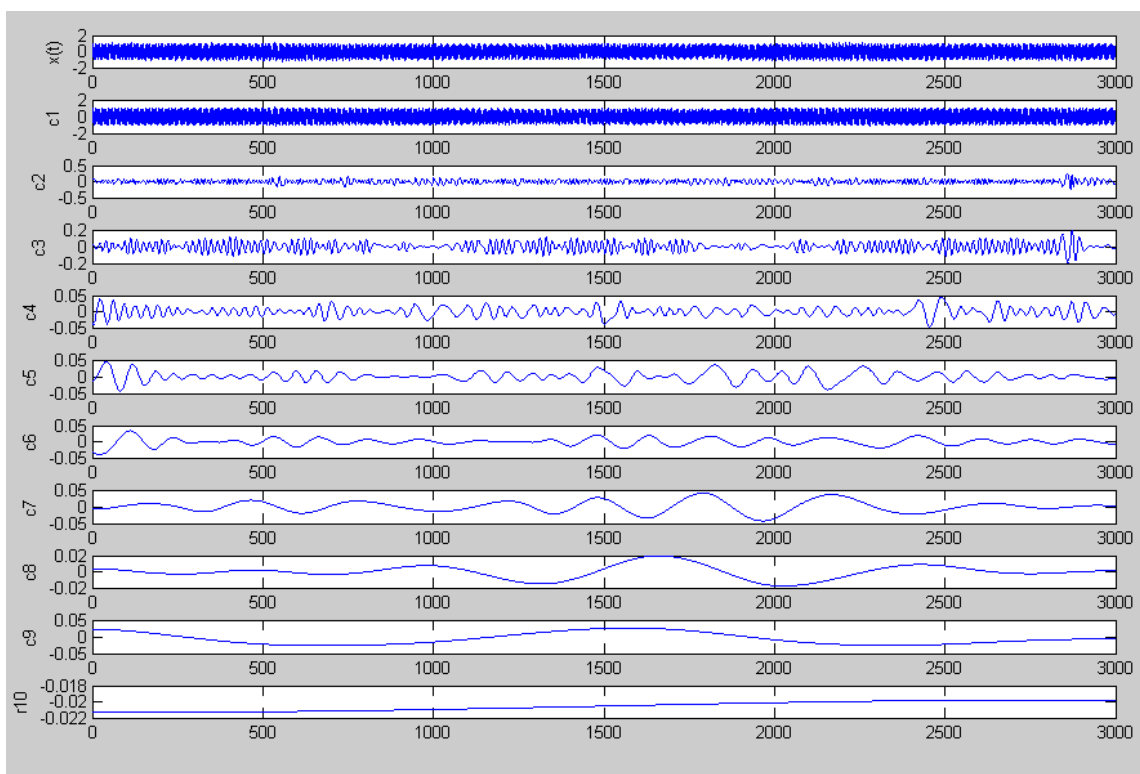


Fig. 6. The original signal and its IMF of the second detection point  $x(t)$  is the original signal,  $c1\sim c9$  is the 9 IMFs,  $r10$  is the surplus

From the Figure 6, we can see obviously each frequency component of output zero-IF of each target layer. We take out segregative frequency component from every layer and reconstruct the lesions information, combining with amplitude feature of back signal.

Microwave spreading in a homogeneous medium, power density attenuate in accordance with the law  $1/R^2$ . In application of BRATUMASS, detected target region is filled with uniform medium of dielectric properties  $\epsilon_0$ , and then add two reflection units of dielectric

properties  $\varepsilon_1$  and  $\varepsilon_2$  into the detected target region. The distances from the two units to the R/T antenna are  $r_1$  and  $r_2$ , respectively.

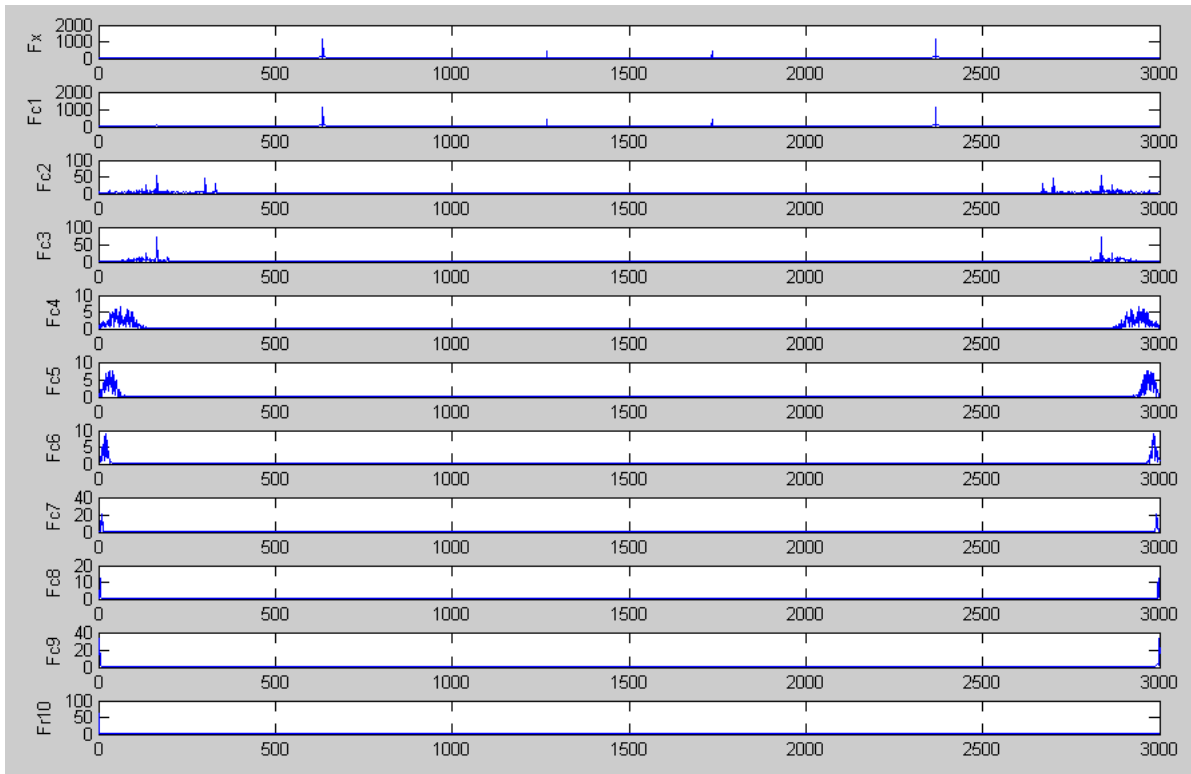


Fig. 7. The Fourier transform of the second detection point  $F_x$  is the Fourier transform of  $x(t)$ ;  $F_{c1} \sim F_{c9}$  is the Fourier transform of the  $c_1 \sim c_9$ ;  $F_{r10}$  is the Fourier transform of  $r_{10}$

The reflection coefficient from the first unit is:

$$\Gamma_1 = \frac{\sqrt{\varepsilon_1} - \sqrt{\varepsilon_2}}{\sqrt{\varepsilon_1} + \sqrt{\varepsilon_2}}, \quad (15)$$

Similarly, the reflection coefficient from the second unit is:

$$\Gamma_2 = \frac{\sqrt{\varepsilon_2} - \sqrt{\varepsilon_0}}{\sqrt{\varepsilon_2} + \sqrt{\varepsilon_0}} \quad (16)$$

When  $|r_1| < |r_2|$  and the incident power is  $P_0$ , the incident power density of the first unit is:

$$S_1 = \frac{P_0}{4\pi r_1^2}, \quad (17)$$

and the incident power density of the second unit is:

$$S_2 = \frac{P_0}{4\pi r_2^2}. \quad (18)$$

The receiving power density from the first unit reflection is:

$$S_{11} = S_1 \times \Gamma_1 \times \frac{1}{4\pi r_1^2} = \Gamma_1 \times \frac{P_0}{16\pi^2 r_1^4} \quad (19)$$

and the receiving power density from the second unit reflection is:

$$S_{22} = S_2 \times \Gamma_2 \times \frac{1}{4\pi r_2^2} = \Gamma_2 \times \frac{P_0}{16\pi^2 r_2^4} \quad (20)$$

In general homogeneous delamination, the greater  $|r|$  is the farther spectrum midline leaves origin.

When  $|r_1| \leq |r_2|$  and are close, meantime, the dielectric properties of two units are different greatly ( $\epsilon_2 > \epsilon_1 > \epsilon$ ), and unit is sorted according to the reflection power density, far distance unit is sorted at front and near distance unit at behind. That is spectrum centerline interleaving to appear. Whether use the malignant tumor tissue dielectric properties 55 ( $\epsilon_2, |r_2|$ ), background dielectric properties 10 ( $\epsilon$ ) and breast tissue (lobule, breast ducts and blood vessels) dielectric properties 30 ( $\epsilon_1, |r_1|$ ) to calculate, then there have:

$$\frac{\Gamma_1}{\Gamma_2} = \frac{r_1^4}{r_2^4} \quad (21)$$

And:  $r_2 \geq \sqrt[4]{1.5} r_1 \approx 1.1 r_1$ . Power spectrum appears overlap after sorted in terms of size of reflection power density, but the actual distances have 1.1 times relationship. Target dielectric properties, which  $|r_2|$  corresponds, is 55 ( $\epsilon_2$ ), this is, the malignant tumor tissue boundary.

The Figure 8 is a typical example of spectrum centerline overlap. From the Figure8, we can see that there are a lot of positions to satisfy spectrum centerline overlap. However, the location satisfied  $r_2 \geq \sqrt[4]{1.5} r_1 \approx 1.1 r_1$  is reduced greatly, as shown in Figure9. So this method can improve detection efficiency.

#### 4. BRATUMASS system signal and data processing

The detection system (BRATUMASS) is re-illustrated in Figure10. BRATUMASS system is a time and distance measurement system, which can determine the distance from breast tumor to antenna by obtaining the time delay between directive wave and scattered wave.(Wang & Yao, 2006) The position of the breast tumor can locate by the distance.

Assume only one tissue interface in the effective detection space. The signal from transmitting antenna is:

$$v_1 = A_c \cos\left(2 * \pi * f_c + 2 * K_c * \int_t H(\tau) d\tau + \theta\right) \quad (22)$$

Where,  $H(\tau)$ =sawtooth( $\tau$ ) is triangular pulse.

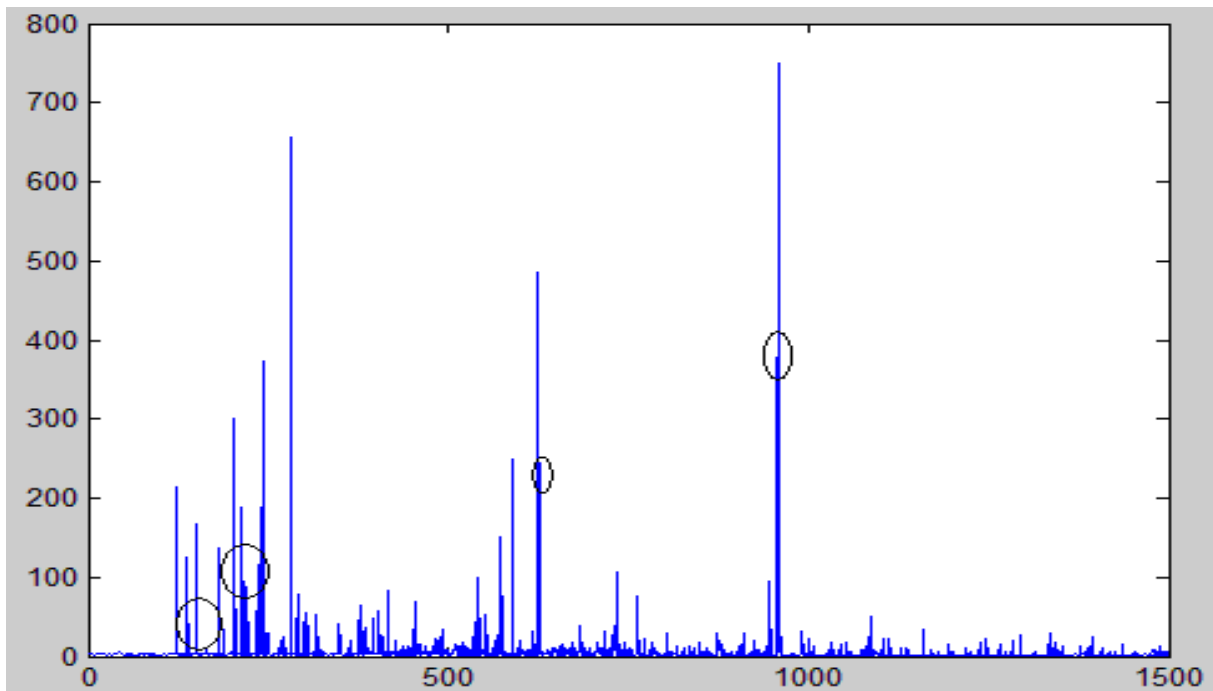


Fig. 8. The typical spectral chart according to the signal energy amplitude after the separation layer of the first patient fourth test signal echo. Abscissa is the signal ordinal number, the vertical axis is the size of the signal period, units are normalized, we can see from the chart a clear spectrum centerline overlap

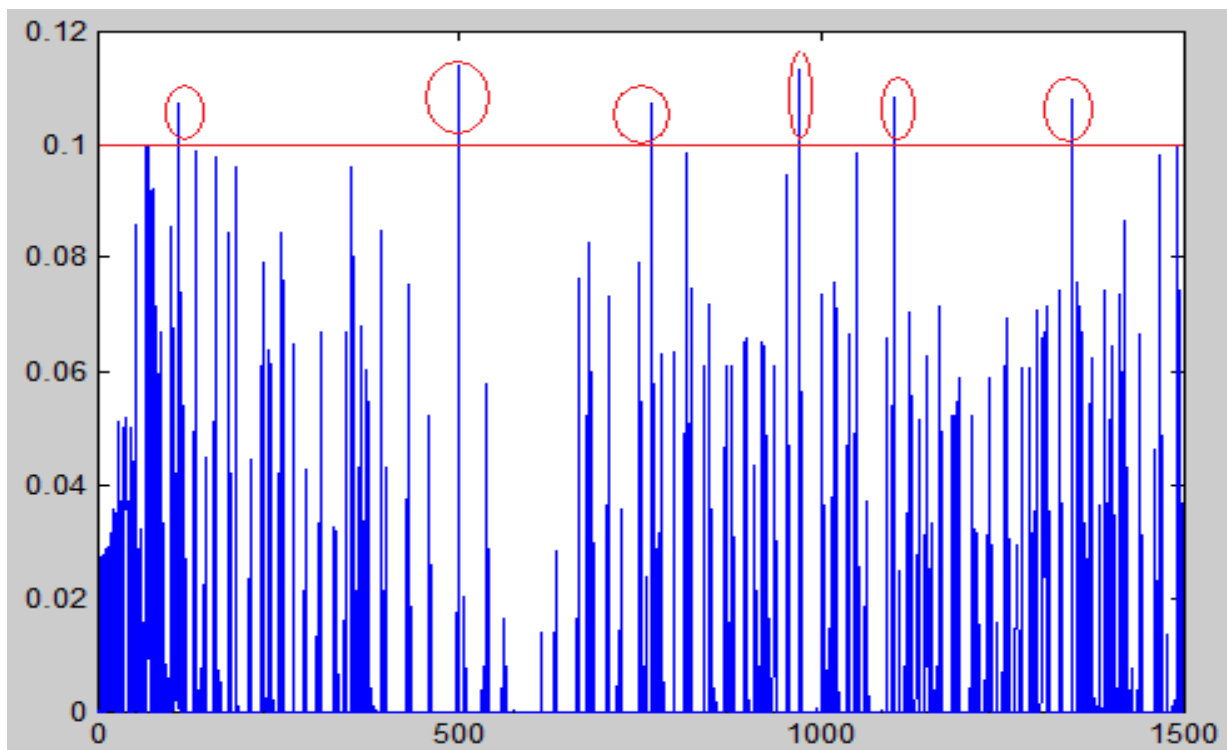


Fig. 9. In the energy spectrum, if the relative difference of energy between two-line is less than 20%, then the location probable is the distortion. Abscissa is the signal ordinal number, the vertical axis is the corresponding relative differences from the overlap line

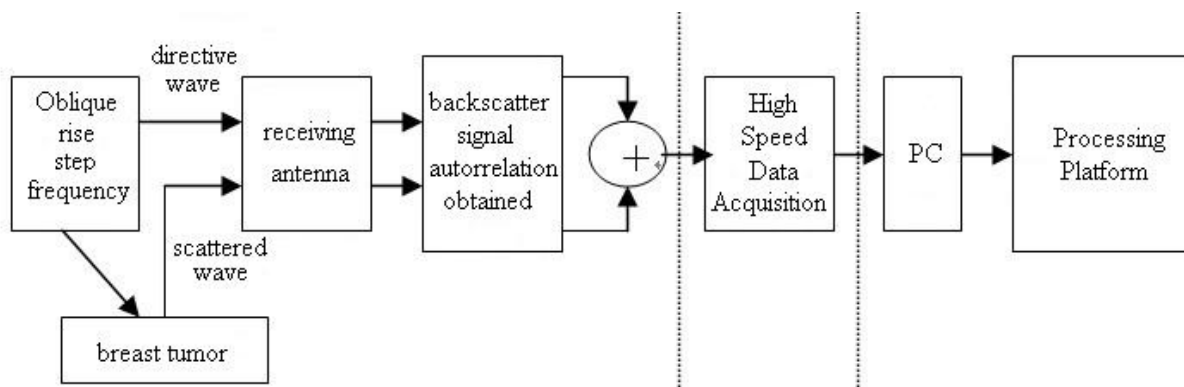


Fig. 10. The diagram of detection system

The received signal from antenna can divide into two parts: one is directive wave from the transmitting antenna; another is scattered wave which is reflected by breast tumor. Propagation distances and propagation times of directive wave and scattered wave are different, because the scattered wave has a time delay  $\Delta t$  related to directive wave. The system can estimate the distance from breast tumor to antenna by obtaining the time delay, then determine the position of the breast tumor by establishing the trajectory equation. (Zheng & Yao, 2005)

BRATUMASS is constructed based on the above-mentioned principle. In the detecting environment of BRATUMASS, the characteristics and delay of single back wave signal is satisfied:  $|\Pi(\tau_i, \omega)| = 2\pi\kappa_i A^2 \delta(\omega - \mu\tau_i)$  after calculation. (Tao, 2011) Where,  $|\Pi(\tau_i, \omega)|$  is the amplitude spectrum of BRATUMASS signal,  $\kappa_i$  is the scattering coefficient of target  $i$ ,  $\tau_i$  is the delay of back wave,  $\mu$  is the FM slope and  $A$  is the amplitude of transmitting signal.

It can be observed that a target which is existed in detection space for single sampling point corresponds to a spectral line in amplitude spectrum of BRATUMASS, whose frequency and amplitude are related to delay (location) and target characteristics, respectively. There have many back wave faces on the rough malignant tissue surface. Then the number of spectral lines in the region of malignant tissue is larger than them in the region of normal tissue. The spectral line represented characteristics of tissue can be determined by analysis the characteristics of back wave.

As early as in 1996, Zhonghua Ma et. al. (Zhang & Xu, 1996) introduced the fractal theory to analyze the karyomorphism of breast cancer and then indicated that the fractal dimension quantitatively describe the degree of irregularity of tumor karyomorphism, which has certain significance in pathology identifying normal and malignant tissue. Overall, the malignancy level is higher, the cell differentiation is worse and the corresponding fractal dimension is larger. By literature, (Hou & Zhu, 2001) we obtained that an object with fractal structure often has a fine structure and very irregular interface, the larger of fractal dimension, the more fine structure of the surface and the more irregular and rougher.

In the actual detection, the back wave not only exists on the malignant tissue surface, but also on other tissues surface. And relatively speaking, the malignant tissue surface is

rougher than normal tissues surface, so the back wave surfaces of malignant tissue are more and relative concentration. This makes the time delays, obtained by total back wave signals, large, which are corresponding to more frequency components after mixing. It is very difficult to separate back waves of malignant tissue from total back waves. However, back waves can be separated by using the characteristics of roughly layered distribution of organism tissue structure. That is to say, different tissue layers are corresponding to certain frequency band in effective frequency domain after mixing. We firstly extract layered structure and then separate and distinguish malignant tissue. That can decrease difficulty of distinguish.

### 5. Wavelet analysis of detection data

Multiresolution analysis is one applications of wavelet analysis. Then, the signals shown in Figure 1 are layered extraction by using wavelet analysis. In wavelet decomposition, the maximum frequency element is seen as one, so the wavelet decomposition of each layers are band-pass or low-pass filters. As close as possible to separate useful information and give detail information for rebuilding nidus, we use db3 wavelet and 11 layers in practice. Figure 11 shows separated results using the wavelet tool box of MATLAB.

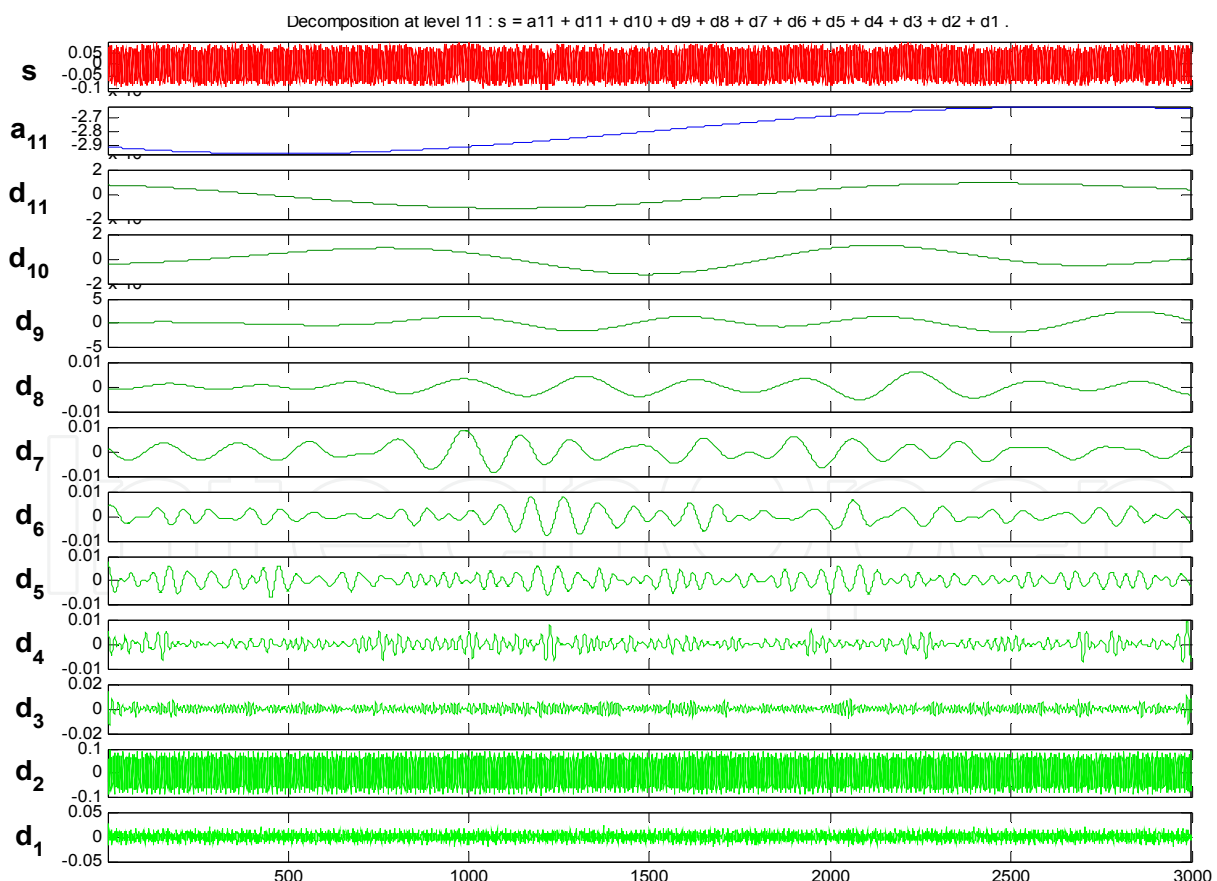


Fig. 11. Separated results of signals of a detection point

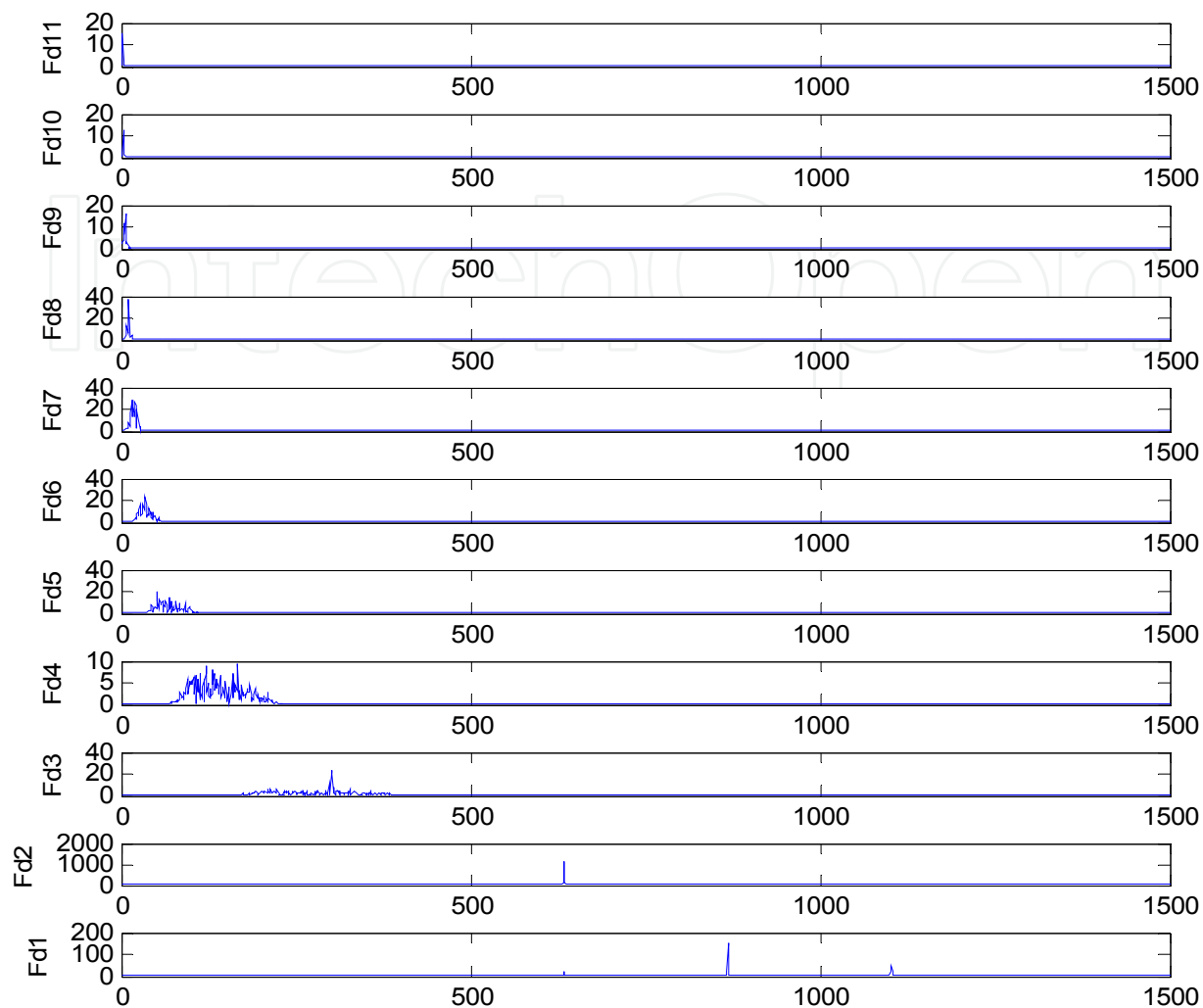


Fig. 12. FFT of each layer

The separated spectrums, which are the FFT of separated layer signals, are shown in Figure 12. The abscissa is corresponding to the spectrum ordinal number in order to remain consistent with latter.

From Figure 12, each layer separates out each frequency component in them own frequency band. Synthesized each layer separation results, spectral lines are ascendingly sequenced according its relative distances, which is the distances between the target and the transmit antenna. Then the information of tissue layers is demonstrated in Figure 13.

As Figure 13 shown, tissue layers are approximate uniformity and continuation in 30mm. There has a more than 2mm discontinuous tissue layer beyond 30mm, which is roughly fit with anatomical structure of breast. When a detection microwave enter into a breast, It firstly encounters a homogeneous fat layer about 1.5cm (3cm/2, microwave have forth and back wave), then it encounters other tissue layers after fat layer.

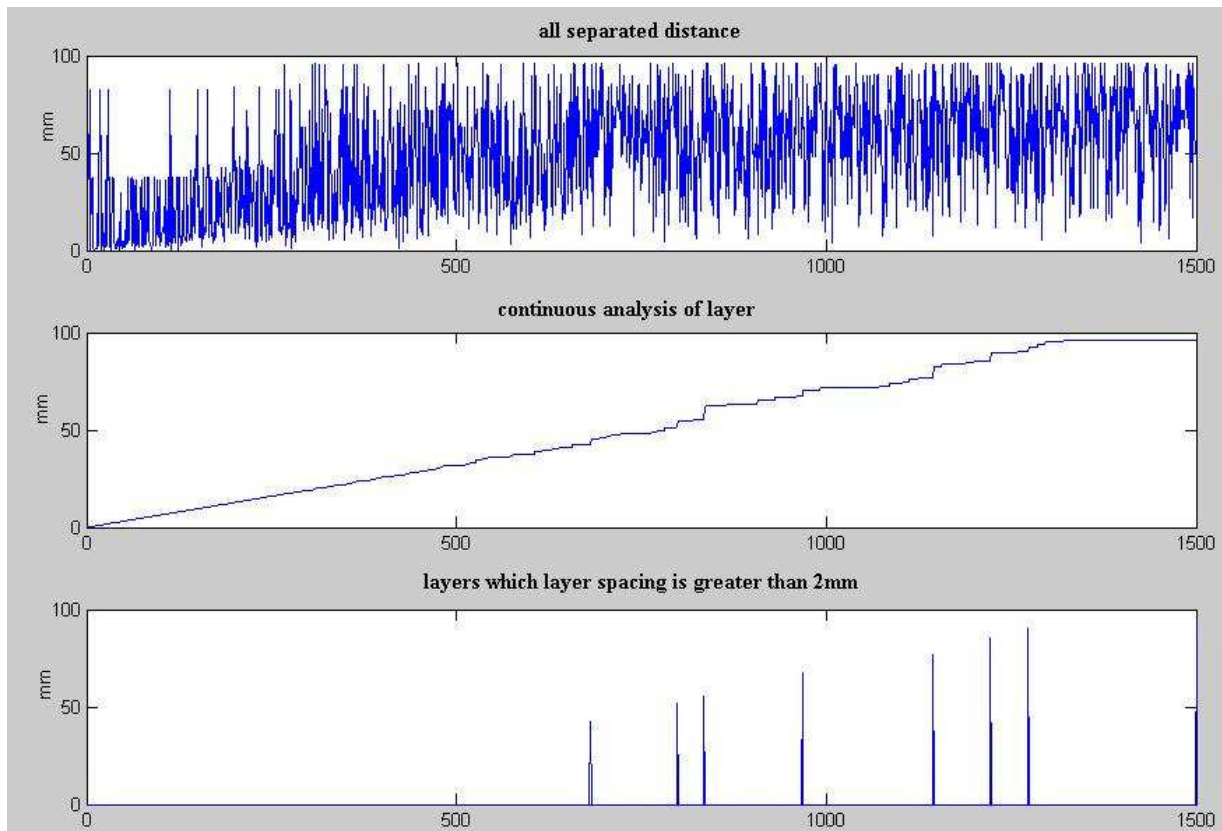


Fig. 13. Relative information of tissues layer

## 6. Discrimination model of characteristics of tissues

Discrimination model of same tissues: we assume that the distribution of same tissues is relatively gathered together as flocculent distribution in detection space. The results of detecting same tissues are basically same. So if the variance of data in detection space is relatively small (meet certain threshold), that space has only one tissue; conversely, that space has several different tissues. That is to say, it would be better of the differentiation of cell development in that space and more kinds of tissues. On the contrary, it would be fewer kinds of tissues.

Assumption of malignant discrimination: the rate of back wave can be used to discriminate the characteristics of tissues. We discriminate malignant tissues by using the adjacent degree between the mean of the spectral lines relatively gathered area and the rate of back wave of malignant tissues.

Consider the following mode function:

$$y(x) = \exp\left(-\frac{(\mu_d(x) - Ld(x))^2}{2\sigma^2}\right) \quad (23)$$

Where,  $\sigma$  is the variance of data window,  $\mu_d$  is the mean of data window,  $d$  is the width of data window,  $x$  is the coordinate of center position of data window,  $Ld(x)$  is the ideal rate of back wave of malignant tissues in that position,  $y(x)$  is the total evaluation index of data window, which is the possibility of the existing malignant tissues in that window area.

Figure 14 illustrates analysis results of sampling data on a case of patient by using this algorithm. The malignant tissue is located the position confirmed by other medical methods as shown in Figure 14. The limit of malignant tissue is approximate 4cm. As shown in the right figure, the malignant tissue is emerged in the distance left antenna from 1cm to 5cm in the fourth sampling point. To the eighth sampling point, the analysis results reveal that the malignant tissue is most probably emerged in the distance left antenna from 5cm to 9cm. Because the sampling antenna is positioned using manual, excursion of mammary glands often occur in sampling. Those factors will increase the probability of error, but the calculation results of the limit of malignant tissue are basic right.

We also used the multi-resolution characteristics of wavelet to get the morphotype of malignant tissue under microwave range sounding signal. Figure 15 showed the processing results of same case of patient (figure 14) from first sample point to fourth sample point.

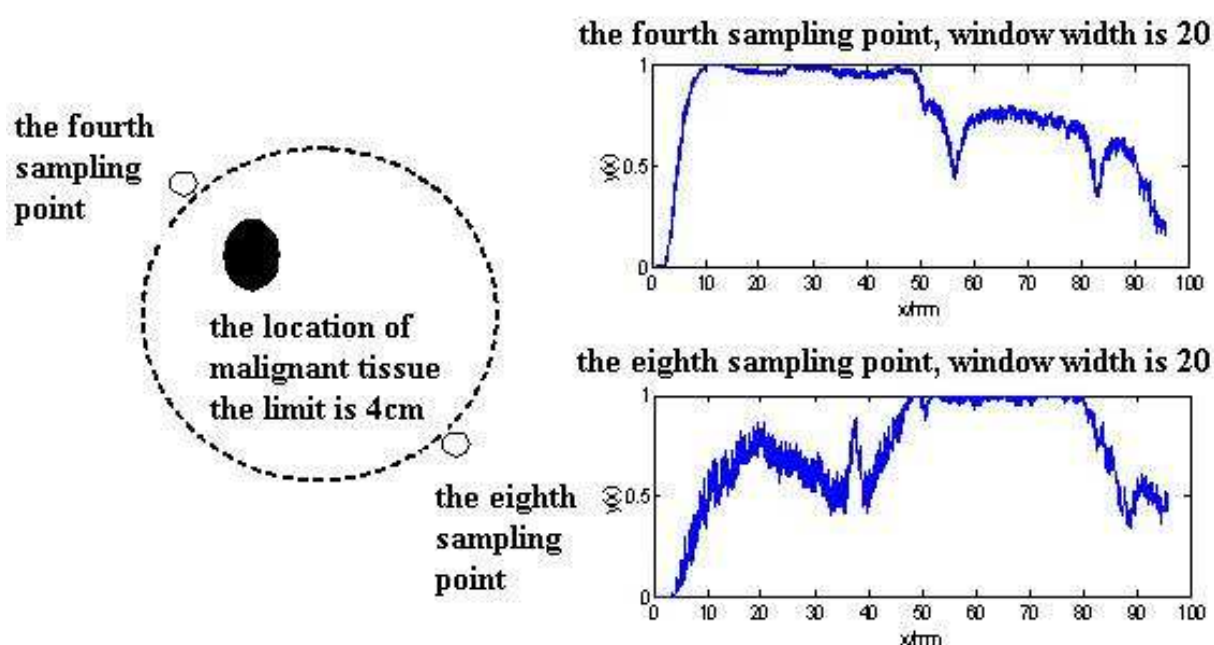


Fig. 14. The position of malignant and the calculation results of malignant degrees in sampling point.

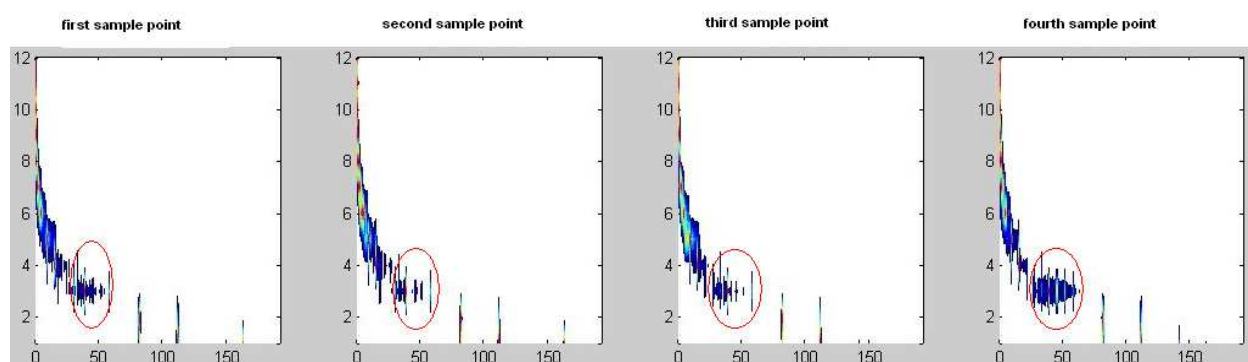


Fig. 15. The morphotype of malignant tissue under microwave range sounding signal

## 7. Conclusion

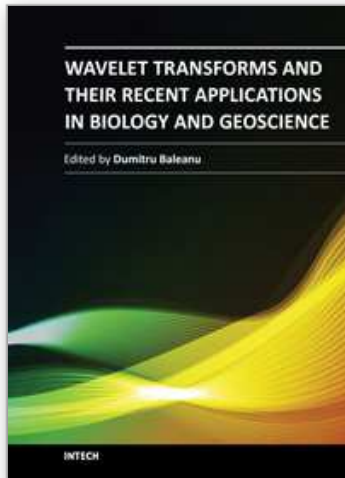
We can achieve the effective analysis to the reflected signals by interface of biological tissues using the multiresolution analysis characteristics of wavelet. At the same time, we can distinguish the malignant tissues and the normal tissues by using the relationship of frequency components which are separated and applying proper discrimination model of tissues. However, we don't detailedly discuss the discriminate threshold in the discrimination model of tissues. In fact, this threshold, in the same tissue and in the same microwave condition, is different at largest microwave response. That threshold needs to be further research.

## 8. Acknowledgments

This work has been performed while Prof. M. Yao was a visiting scholar in Michigan State University, thanks to a visiting research program from Prof. Erik D. Goodman. M. Yao would also like to acknowledge the support of Shanghai Science and Technology Development Foundation under the project grant numbers 03JC14026 and 08JC1409200, as well as the support of TI Co. Ltd through TI (China) Innovation Foundation.

## 9. References

- Hou, Rong-tao; Zhu, Fei. J (2001) *Fractal theory and its significance*. China Computer & Communication 2001.1:196
- Huang, N. E., etc R. (1998). *The empirical mode decomposition and the Hilbert spectrum for non-linear and non-stationary time series analysis*. pp. 903-995 Proc. R. Soc, London, 454 (A)
- Tao, Zhi-fu. R.(2011) *Investigation on the methodologies of near-field microwave echo imaging integrity*. The Ph.D. Thesis of East China normal university, 2011.
- Wang, Cui; Yao, Meng. J (2006) *Practical Near-field Microwave Sounding Image Method for Early-stage Breast Cancer* Chinese Journal of Scientific Instrument. 2006(S3)
- Xu, Kaiye; Tang, Aorong; M. (1996) *The Imaging Diagnosis of Mammary Gland Disease*. Shanghai Science and Technology Press, Shanghai China
- Zhang, Zhong-hua; Xu Yuan-ding. J(1996) *Fractal Analysis of Cell Nucleus of Breast Carcinoma*. Tumor. 1996,16(2):63
- Zheng, Shijun; Yao, Meng. J (2006) *HFSS Simulation on the Microwave Sounding for Mammary Tumor* Chinese Journal of Scientific Instrument. 2005(S1)



## **Wavelet Transforms and Their Recent Applications in Biology and Geoscience**

Edited by Dr. Dumitru Baleanu

ISBN 978-953-51-0212-0

Hard cover, 298 pages

**Publisher** InTech

**Published online** 02, March, 2012

**Published in print edition** March, 2012

This book reports on recent applications in biology and geoscience. Among them we mention the application of wavelet transforms in the treatment of EEG signals, the dimensionality reduction of the gait recognition framework, the biometric identification and verification. The book also contains applications of the wavelet transforms in the analysis of data collected from sport and breast cancer. The denoting procedure is analyzed within wavelet transform and applied on data coming from real world applications. The book ends with two important applications of the wavelet transforms in geoscience.

### **How to reference**

In order to correctly reference this scholarly work, feel free to copy and paste the following:

Meng Yao, Zhifu Tao and Zhongling Han (2012). The Detection Data of Mammary Carcinoma Processing Method Based on the Wavelet Transformation, *Wavelet Transforms and Their Recent Applications in Biology and Geoscience*, Dr. Dumitru Baleanu (Ed.), ISBN: 978-953-51-0212-0, InTech, Available from: <http://www.intechopen.com/books/wavelet-transforms-and-their-recent-applications-in-biology-and-geoscience/data-analysis-of-microwave-breast-tumor-detection-system-with-wavelet-transform>

**INTECH**  
open science | open minds

### **InTech Europe**

University Campus STeP Ri  
Slavka Krautzeka 83/A  
51000 Rijeka, Croatia  
Phone: +385 (51) 770 447  
Fax: +385 (51) 686 166  
[www.intechopen.com](http://www.intechopen.com)

### **InTech China**

Unit 405, Office Block, Hotel Equatorial Shanghai  
No.65, Yan An Road (West), Shanghai, 200040, China  
中国上海市延安西路65号上海国际贵都大饭店办公楼405单元  
Phone: +86-21-62489820  
Fax: +86-21-62489821

© 2012 The Author(s). Licensee IntechOpen. This is an open access article distributed under the terms of the [Creative Commons Attribution 3.0 License](#), which permits unrestricted use, distribution, and reproduction in any medium, provided the original work is properly cited.

IntechOpen

IntechOpen